Crystal Face Anisotropy of Propylene Oxidation on Molybdenum Trioxide

Shigeo Ted OYAMA†
Catalytica, 430 Ferguson Drive, Building 3, Mt. View, CA 94305, U.S.A.
(Received February 23, 1987)

Samples of MoO_3 consisting of unsupported oriented crystallites exposing primarily the (010) plane and of randomly oriented powders were used to study the partial oxidation of propylene and allyl iodide. The materials were characterized by scanning electron microscopy, X-ray diffraction, infrared spectroscopy, laser Raman spectroscopy, temperature programmed desorption of ammonia and surface area measurements. The unoriented powders were twice as active as the oriented crystallites in the oxidation of propylene, but both were similar in activity in the oxidation of allyl iodide. Thus, the reactions depended only slightly on the structure of the MoO_3.

The concept of structure-sensitivity has been useful in the study of the catalytic activity of metals, but has been little exploited in the case of nonmetallic catalysts such as sulfides or oxides. The bonding in nonmetals is more highly localized and directional than on metals. Thus, on nonmetals geometrical constraints for surface intermediates are likely to be greater than on metals, and surface structure might be expected to play a greater role in nonmetal reactivity. Investigations of the catalytic activity of different faces of nonmetal single crystals were pioneered by Tanaka and Okuhara[1-3] who found that isomerization and hydrogen exchange of olefins proceed on the edge planes of MoS_2 whereas the isomerization of 2-methyl-1-butene occurs on the basal planes. Berlowitz and Kung[4] report that dehydrogenation of 2-propanol to acetone on zinc oxide proceeds three to five times faster on polar crystal faces where zinc atoms are exposed than on similar polar faces where oxygen is exposed.

Structure-sensitive reactions may be defined to be those whose rates change appreciably with the atomic structure of the surface.[5-8] There is no clear dividing line between structure-sensitive and insensitive reactions, although the former on metals often show activity differences of tens, hundreds, it not thousands, between samples of different structure. Structure-sensitive reactions studied over different crystalline faces of a solid should also show pronounced reactivity differences, and this will be referred to as crystal face anisotropy.

In recent years there have been a number of attempts to study this topic, with MoO_3 receiving considerable attention. Volta et al., have investigated the oxidation of propylene on oriented crystallites of MoO_3 supported on graphite[9-13] and have concluded that the various faces catalyze different reactions. They correlated small changes in selectivity to the amounts of different exposed crystal faces determined from microphotographs and inferred that for propylene oxidation the (010) basal face produces exclusively carbon oxides, while the (100) and (101) edge faces produce acrolein.[13] The present paper seeks to examine these conclusions and reopen the question of the crystal face anisotropy of the reaction. The investigation is carried out on oriented crystallites of MoO_3, materials similar to the ones used by Volta et al., except that they leave out the support and, therefore, its possible influence.

Tatibouët and Germain have used the same system, unsupported crystallites of MoO_3 preferentially exposing different faces, in the oxidation of methanol[14] and ethanol.[15,16] These investigators concluded that the (010) face carries active centers for the oxidative dehydrogenation of methanol to formaldehyde. Ohuchi et al., have compared the temperature-programmed reaction and desorption of methanol from MoO_3 single crystals and powder.[17,18] These investigators found formaldehyde desorbing from the powder and only methanol desorbing from the (010) face of the single crystal. From this they reached an opposite conclusion from that of Tatibouët and Germain, namely, that the (010) face is inactive for the partial oxidation of methanol. These studies on MoO_3 have inspired theoretical work by Ziólkowski[19] and by Allison and Goddard.[20] The latter propose that the molybdenum dioxo groups found on the (010) plane are particularly effective for the oxidation of methanol, thus supporting the findings of Tatibouët and Germain.

The unit cell of MoO_3 is orthorhombic with lattice parameters a_o=396.28±0.07 pm, b_o=1385.5±0.3 pm, and c_o=369.64±0.06 pm.[21] Figure 1 illustrates the crystal structure. The structure consists of double layers of MoO_6 octahedra held together by covalent forces in the (100) and (001) directions, but by van der Waals forces in the (010) direction. As a consequence, large MoO_3 crystallites have elongated slab-like habits preferentially exposing the (010) direction.

Experimental

Reagent grade MoO_3 powder (Mallinckrodt, 99.95%) was used as received. Propylene (Linde, 99.0%) was purified by passage through a reduced Ni/SiO_2 trap and through a Molecular Sieve 3A trap. Allyl iodide (Aldrich, 98%), high purity ammonia (Linde, 99.995%), oxygen (Linde, 99.99%), nitrogen (Linde, 99.998%), and helium (Linde, 99.995%) were used without further purification.

† Present address: Dept. of Chemical Engineering, Clarkson Univ., Potsdam, New York 13676, U.S.A.

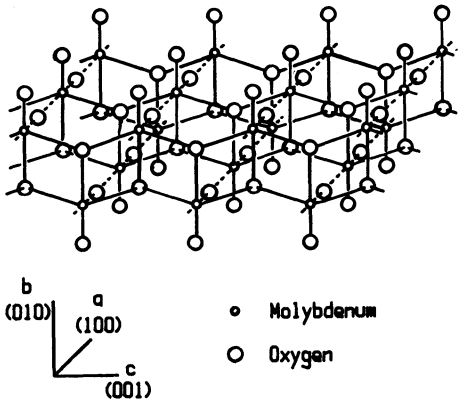

Fig. 1. Structure of orthorhombic MoO_3.
Terminal oxygen atoms extend in the (010) direction, two-fold coordinate oxygen atoms in the (100) direction and three-fold coordinate oxygen atoms in the (001) direction.

X-Ray diffraction patterns were taken with a Norelco 12206/7 spectrometer using Cu Kα radiation. Samples were lightly pressed onto a shallow indentation in an aluminium sample holder to provide a flat 1 cm×1 cm surface. Infrared spectra of the powder were taken with a Perkin Elmer 1330 spectrometer with about 0.1 wt% of the sample pressed in KBr pellets. Laser Raman spectra were obtained with a Cary 81 spectrometer equipped with 90° optics and using the 632.8 nm output of a 50 mW He–Ne laser. Scanning electron micrographs were measured with a JEOL JSM 35 microscope with samples sprayed with a palladium gold coating to prevent charging effects. Surface area and temperature-programmed desorption measurements were carried out in a flow system equipped with a single-filament TC detector (Hewlett-Packard 19302-60530), with samples treated in flowing He at 473 K prior to measurement. Absolute absorbate amounts were obtained by comparing the areas under the desorption peaks to those under standard calibration pulses from a sampling valve. Single-point BET areas were obtained by equilibrating the sample with a 30 mol% N_2 in He stream at liquid nitrogen temperatures followed by flash desorption of the adsorbed nitrogen. Ammonia TPD spectra were obtained by saturating samples held at 273 K with NH_3, purging the samples in the He carrier and then monitoring the desorption peaks as the temperature was raised linearly at 0.17 K s^{-1}. Because of the use of a thermal conductivity detector the possibility of NH_3 oxidation as well as desorption cannot be ruled out. However, the technique was used primarily to show differences between samples.

Reactivity measurements were carried out in two separate reactor systems of almost identical design which could be used in both flow and pulse modes. The only difference between the systems was that for analysis of products one used an on-line gas chromatograph (Hewlett-Packard 5880 GC) whereas the other used an on-line mass spectrometer (Hewlett-Packard 5995 GC-MS). The reactor with the gas chromatograph was used in a flow mode for the propylene oxidation work, whereas the reactor with the mass spectrometer was used primarily in a pulse mode for the allyl iodide oxidation investigations. However, propylene oxidation data taken in one system could readily be reproduced in the other. The gas chromatograph used an octane on Porasil C column and an OV-101 column which were respectively connected to a TC and a FI detector. The mass spectrometer simultaneously monitored the ion masses of all product species. Injections of pulses of N_2 as a standard allowed the calibration of the sensitivity of the mass spectrometer prior to each run and, thus, the quantification of the products of the reaction. For the pulse reaction an average reaction rate was obtained by integrating the concentration of each species through the duration of each pulse (60 s).

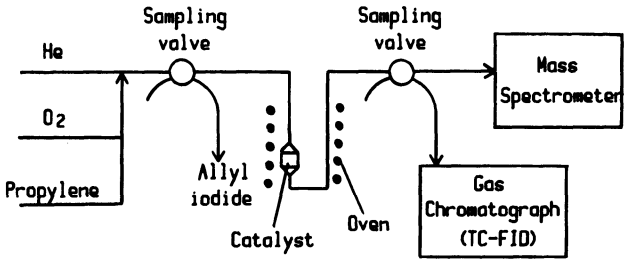

Fig. 2. Schematic diagram of the flow reactor apparatus.

A schematic diagram common to both flow systems is presented in Fig. 2. Electronic mass flow controllers (Brooks 5850) delivered gases in precise proportions. For the allyl iodide experiments a sampling valve injected pulses of He carrier gas containing the vaporized liquid reactant. The catalysts were in packed beds held in Pyrex or 316 stainless steel tubes by either sintered glass frits or packed glass wool. Furnaces surrounded the tubes and heated them. Thermocouples clamped to the outside of the tubes monitored the temperature of the beds. Heated transfer lines led the effluent to the analyzers.

Table 1 summarizes the conditions at which the steady-state propylene oxidation data were obtained. Flow rates are expressed in units of μmol s^{-1} which can be converted to units of cm^3 (NTP) min^{-1} by multiplication by 1.5. The contact time is defined as the bed volume divided by the volumetric flow rate. To compare accurately the reactivity of the needles and powder, quantities of catalyst corresponding to the same total surface area of 0.18 m^2 were employed. Furthermore, since the MoO_3 powder was denser than the needles, the former was diluted with inert, acid-washed ground quartz to achieve equal bed volumes of 2.2 cm^3. Rates are reported as areal rates, i.e., per unit surface area.

The allyl iodide oxidation data were obtained with amounts of catalyst and conditions similar to those employed for the propylene oxidation measurements. The flow rate of the helium and oxygen were 60 and 6 μmol s^{-1}, and the delivery rate of allyl iodide was 0.13 μmol s^{-1}. This delivery rate corresponds to the injection of pulses containing 7.6 μmol of allyl iodide every 60 s.

Neither reactor material nor shape had an influence on the results except at the highest temperatures (>800 K). Above this temperature blank runs with acid washed quartz showed there was some contribution to the reactivity from the reactor or from homogeneous gas phase reactions. All conclusions from this study will be drawn from the lower

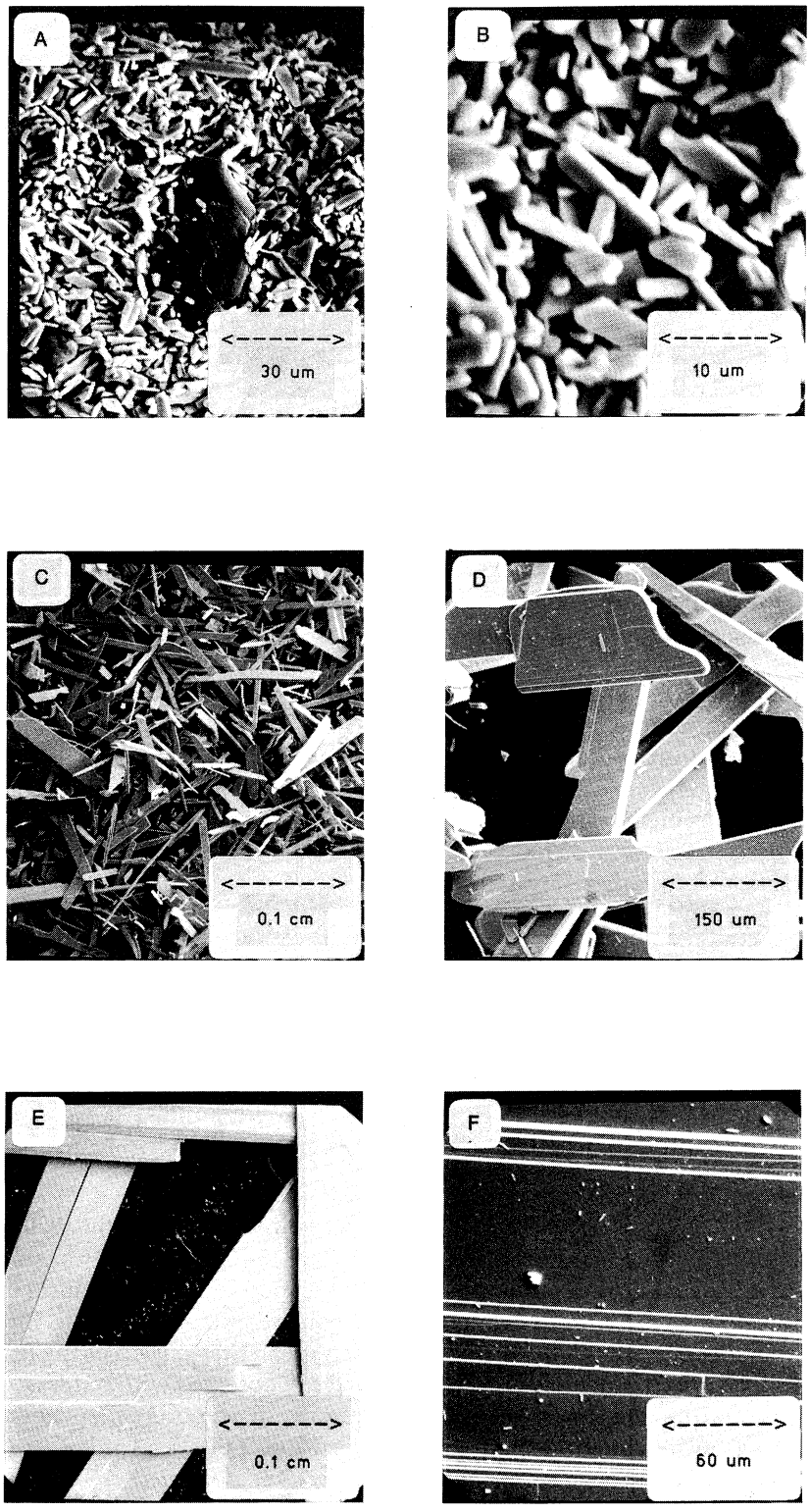

Fig. 3. Scanning electron micrographs of MoO_3 samples.
High and low magnification pictures of the powder (a and b), needles (c and d), and slabs (e and f).

Table 1. Reaction Conditions for Propylene Oxidation

Temperature = 300—900 K	Amount of catalyst = 0.18 m^2
Pressure = 101 kPa	Bed volume = 2.2 cm^3
Flow rate He = 60 $\mu mol\ s^{-1}$	Contact time = 1.3 s
Flow rate O_2 = 3—12 $\mu mol\ s^{-1}$	Conversion = 0—90%
Flow rate C_3 = 3 $\mu mol\ s^{-1}$	

Table 2. Physical Properties of the MoO_3 Samples

Sample	Dimension	Basal plane	Edge plane	Surface area/$m^2\ g^{-1}$ Calculated	Measured
Powder	1×3×3 μm	60	40	0.72	0.81
Needle	10×100×700 μm	90	10	0.047	0.080
Slab	0.03×0.2×3 cm	90	10	0.0025	—

temperature, lower conversion region of the data. At all conversions carbon mass balances of 100±5% were obtained.

Results

Synthesis of MoO_3 Single Crystals. Single crystals of MoO_3 were prepared following the method reported by Wanklyn,[22] consisting of vaporizing a MoO_3 powder and condensing the product crystals a short distance away. Approximately 50 g of MoO_3 were loaded in a shallow, covered alumina crucible which was placed in a temperature-controlled oven. Unlike in the work of Wanklyn who used a constant temperature of 993 K, the temperature here was allowed to oscillate between 987 and 997 K. This resulted in the formation of larger crystallites, probably by an Ostwald ripening process.

Different products were obtained depending on the duration of the synthesis. From an initial micrometer-sized powder, hundred-fold larger needle-shaped crystallites could be collected after 40 hours. After 150 hours even larger, centimeter-sized single crystal slabs were formed. In the following sections these materials will be simply referred to as powders, needles, and slabs. Because of the low surface area of the slabs, the catalytic work will concentrate on the powder and needles.

Characterization. Figure 3 shows scanning electron micrographs of the three samples at various magnifications that indicate the variation in external morphology of the powder, needles, and slabs. Table 2 summarizes the physical characteristics of the samples. The size of the crystallites in the samples is estimated without carrying out a statistical analysis. The dimensions are used to roughly calculate the relative proportions of basal and edge planes, as well as the surface areas. The measured surface areas are also reported.

Figure 4 compares the X-ray diffraction patterns of the MoO_3 powders and needles. The MoO_3 powder displays a pattern characteristic of randomly oriented crystallites. The needles, however, exhibit a pattern

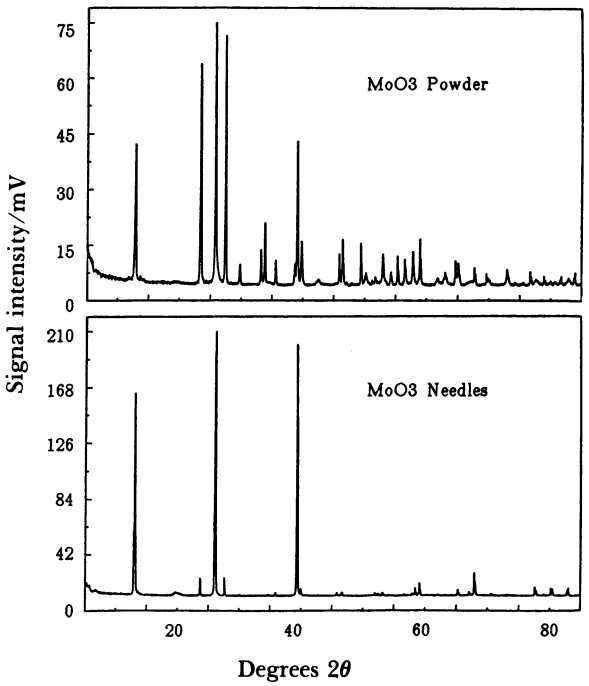

Fig. 4. X-Ray diffraction patterns of MoO_3 samples. Top, MoO_3 powder. Bottom, MoO_3 needles.

with strong intensity in the (020) family of reflections.

Figure 5 shows the transmission infrared and Raman spectra of molybdenum trioxide powder taken at room temperature. It is interesting to note the much greater resolution of the Raman spectra. This is generally observed with oxides.

Figure 6 reports the temperature-programmed desorption (TPD) profiles of ammonia from the needles and powder. The needles had a single desorption peak at 330 K whereas the powder had two desorption peaks at 320 and 430 K. Integration of the areas under the desorption peaks allowed the calculation of the surface number density of ammonia molecules absorbed. These values were $4.0\times10^{19}\ m^{-2}$ for the needles and $6.7\times10^{19}\ m^{-2}$ for the powder.

Reactivity Results. Figures 7 and 8 present the

propylene oxidation data for the needles and powder at various oxygen partial pressures. The only products that were detected were acrolein and carbon dioxide. For both catalysts the rate of carbon dioxide production per unit surface area was similar. As the temperature was raised, this rate increased to a plateau and then slowly decreased. The rate in the region of the plateau varied with the first order of the oxygen

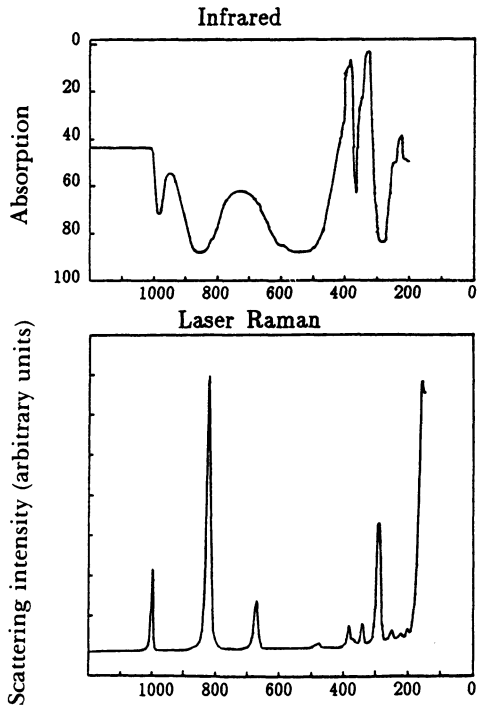

Fig. 5. Vibrational spectra of MoO_3 powder.
Top, infrared spectrum. Bottom, laser Raman spectrum.

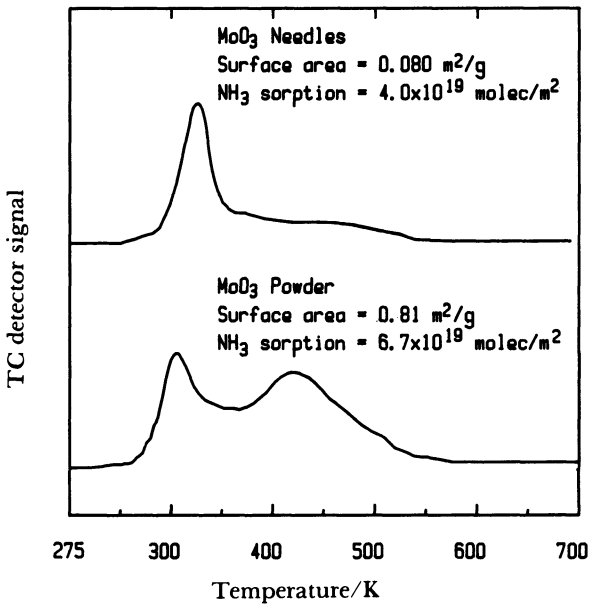

Fig. 6. Ammonia temperature programmed desorption spectra of the MoO_3 needles and powder.
Top, MoO_3 needles. Bottom, MoO_3 powder.

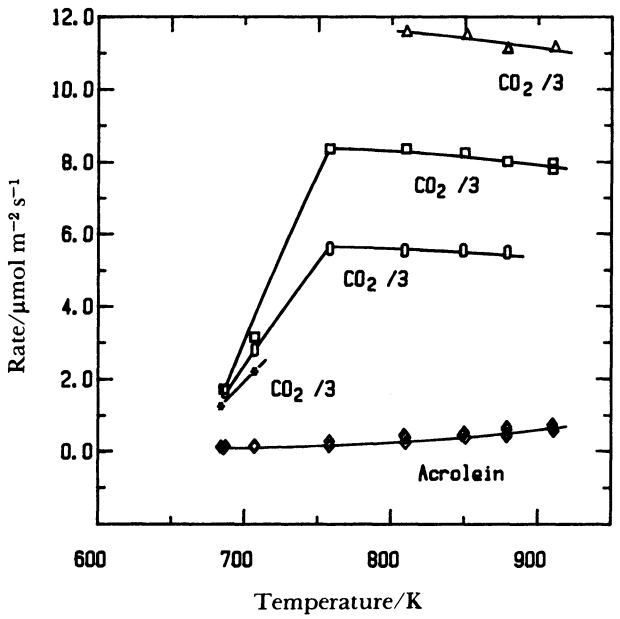

Fig. 7. Steady-state propylele oxidation on MoO_3 needles.
Total pressure=101 kPa. Partial pressure propylene= 4 kPa, partial pressure oxygen=4 kPa (✳), 8 kPa (○), 12 kPa (□), and 16 kPa (△), partial pressure helium= balance. Acrolein production (◇) was independent of oxygen pressure.

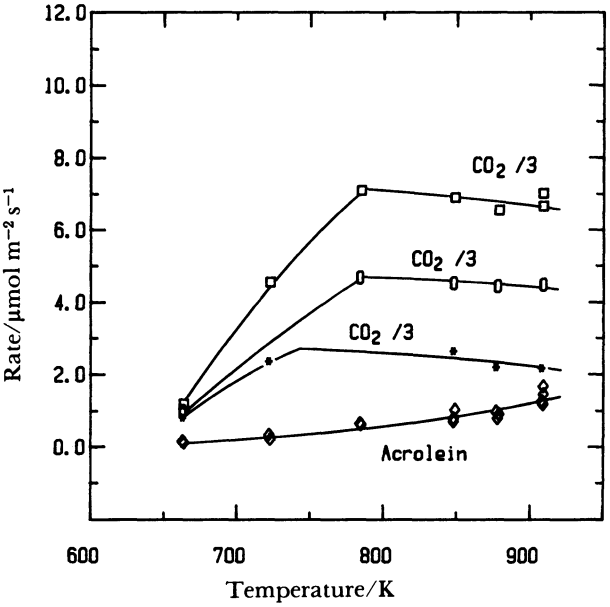

Fig. 8. Steady-state propylene oxidation on MoO_3 powder.
Total pressure=101 kPa. Partial pressue propylene= 4 kPa, partial pressue oxygen=4 kPa (✳), 8 kPa (○), and 12 kPa (□), partial pressure helium=balance. Acrolein production (◇) was independent of oxygen partial pressure.

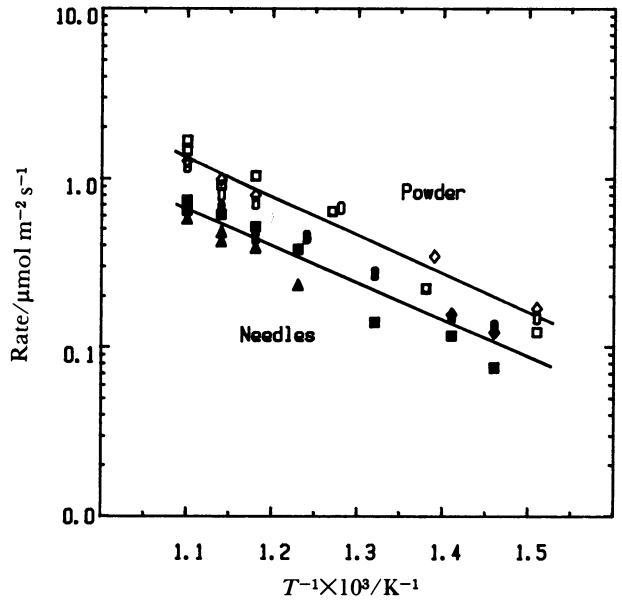

Fig. 9. Steady-state propylene oxidation to acrolein on MoO_3 powder and needles.
Total pressure=101 kPa. Partial pressure propylene= 4 kPa, partial pressure oxygen=4 kPa (◇), 8 kPa (○), 12 kPa (□), and 16 kPa (△), partial pressure helium=balance. Powder=open symbols, needles= filled symbols.

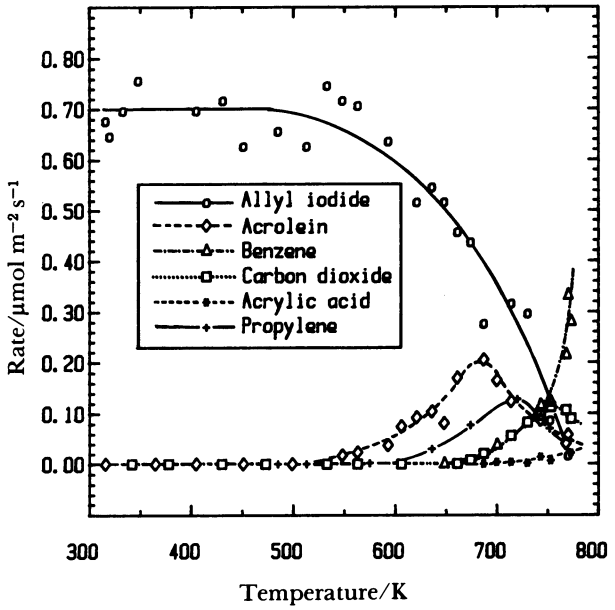

Fig. 10. Allyl iodide pulse oxidation on MoO_3 needles.
Total pressure=101 kPa. Partial pressure oxygen= 9 kPa, partial pressure helium=balance. Allyl iodide pulse size=7.6 μmol.

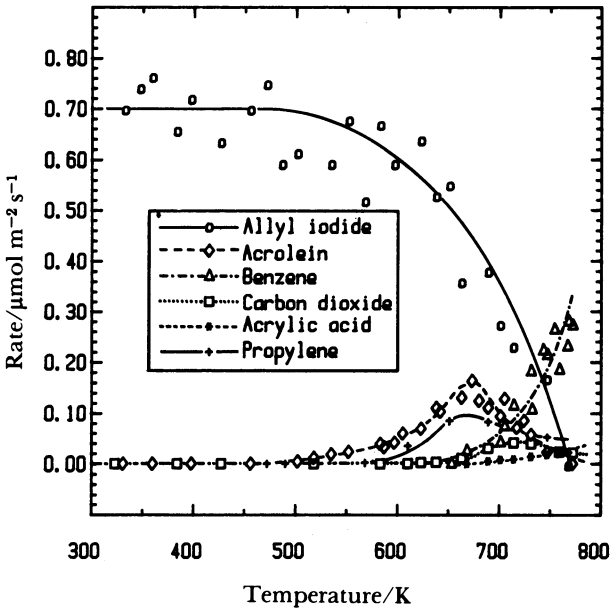

Fig. 11. Allyl iodide pulse oxidation on MoO_3 powder.
Total pressure=101 kPa. Partial pressure oxygen= 9 kPa, partial pressure helium=balance. Allyl iodide pulse size=7.6 μmol.

partial pressure, $v_{CO_2}=kP_{O_2}^{1.0}$.

The data for the rate of acrolein production in Figs. 7 and 8 are presented in Arrhenius form in Fig. 9. The rate was independent of oxygen partial pressure, $v_{ACR}=kP_{O_2}^{0}$, and was uniformly higher by a factor of about 2 on the powder than on the needles. The apparent activation energy, E_{APP}, was the same for both samples within experimental error (±2 kJ mol^{-1}), 43 kJ mol^{-1} for the powder and 42 kJ mol^{-1} for the needles.

The allyl iodide oxidation data taken in a pulse mode are presented in Figs. 10 and 11. The oxidation produced a number of products, acrolein, benzene, carbon dioxide, acrylic acid and propylene. The behavior of the needles and the powder was very similar, although at higher conversions the needles produced more acrolein than the powder (0.21 vs. 0.16 μmol m^{-2} s^{-1}).

Discussion

Structure of the Catalysts. Transmission infrared spectroscopy and laser Raman spectroscopy characterize the bulk of the MoO_3 crystallites; scanning electron microscopy and X-ray diffraction reveal the external macroscopic morphology and orientation; and TPD of ammonia gives information about their surface.

The scanning electron micrographs of the MoO_3 powder and needles show that the samples have different morphologies. The powder consists of small crystallites with little tendency to expose a preferred orientation. The needles consist of larger crystallites with a substantial proportion of flat faces. The X-ray

diffraction pattern of the needles shows that the flat faces are those perpendicular to the (010) direction. The high intensity of the diffraction peaks in that direction are due to preferential orientation of the flat crystallites in the plane of the sample holder.

The surface areas of the materials was calculated from the average size of the crystallites obtained from the scanning electron micrographs. This was done by first calculating the number of such crystallites in one gram using the bulk density of MoO_3 (4.692 g cm^{-3}), and then calculating the corresponding geometric area of the crystallites using their known dimensions. This gave calculated surface areas for the powder and needles of 0.72 and 0.047 $m^2 g^{-1}$. These are in reasonable agreement with the measured values of 0.81 and 0.080 $m^2 g^{-1}$. The lower calculated value for the needles is probably due to underestimating the number of smaller crystallites.

The TPD spectra of ammonia provide direct evidence that the surfaces of the samples are significantly different and that, hence, the samples are appropriate for investigating crystal face anisotropy. The needles show a single desorption feature at 330 K, whereas the powder shows a similar feature at 320 K and a broad desorption peak centered at 430 K. The peak at 320—330 K in both samples is probably due to desorption of ammonia from the basal (010) planes. For the powder the broad peak at 430 K is probably due to the presence of a substantial proportion of other planes, as was shown by the scanning electron micrographs. The surface number density of adsorbed ammonia was 4.0×10^{19} m^{-2} for the needles and 6.7×10^{19} m^{-2} for the powder. The number density of exposed surface molybdenum atoms on the low index planes of MoO_3 are 7.81×10^{18} m^{-2} for the (100) plane, 6.83×10^{18} m^{-2} for the (010) plane and 7.28×10^{18} m^{-2} for the (001) plane. Because of the MoO_3 stoichiometry the total surface atom density, including oxygen atoms, will be roughly four times the above values. Thus, the quantity of adsorbed ammonia corresponds approximately to a monolayer.

General Aspects of the Allylic Oxidation of Propylene. There are two features of the selective oxidation of propylene on molybdate catalysts that are generally accepted. The first feature is that the rate-determining step in the reaction is the abstraction of an allylic hydrogen atom to form an adsorbed allyl radical.[23-27] This will be discussed in more detail below. The second feature is that the oxygen species responsible for selective oxygenation is lattice oxygen.[26-29] Absorbed oxygen species, especially those that are electrophilic in nature (O_2^-, O_2^{2-}, O^{2-}), are thought to be responsible for complete oxidation.[30,31]

Our results for the propylene oxidation reaction agree with the above view. The lack of dependence of acrolein formation on oxygen partial pressure is consistent with the participation of lattice oxygen in the reaction. Similarly, the dependence of carbon dioxide formation on oxygen partial pressure is consistent with the reaction of propylene or some propylene-derived species with absorbed oxygen. Indeed, it is precisely in the region where CO_2 is observed, 700—900 K, that $^{16}O_2$–$^{18}O_2$ exchange, and thus probably chemisorption, on MoO_3 is found to begin.[32,33] The observation in this study of a decrease in the rate of formation of CO_2 in the region of the plateau can be explained by the expected decrease in the amount of chemisorbed oxygen as the temperature increases.

Molybdenum trioxide is generally described as a selective but inactive catalyst for propylene oxidation. In this study the low selectivity obtained is probably due to the high temperatures employed. The activation energy obtained for the production of acrolein, close to 43 kJ mol^{-1}, is low. This is understandable as the value is an apparent activation energy that includes contributions from a number of reactions, including the further oxidation of acrolein.

Allyl Iodide Oxidation. The results obtained in this study for the oxidation of allyl iodide are similar to those found in previous examinations of the reaction by the group of Haber[34] and by Burrington and Grasselli.[35] In the present work, however, provision was taken to cofeed oxygen so as to maintain the surface of the catalyst oxidized. In molybdenum trioxide alteration of the structure on reduction occurs by a crystallographic shear mechanism[36,37] in which corner-sharing octahedra become

Table 3. Summary of Results on Propylene Oxidation

Steady-state selectivity (%) (This work)			
T=673 K Conversion=9%			
	Acrolein	CO_2	Others
(020) MoO_3 crystallites	3	97	—
Non-oriented MoO_3 crystallites	6	94	—
Initial selectivity (%) (Refs. 10, 11)			
T=648 K Conversion<1%			
	Acrolein	CO_2	Others
(020) MoO_3 crystallites	4	94	1
Non-oriented MO_3 crystallites	10	86	4

Table 4. Summary of Results on Allyl Oxidation

MoO_3 crystallites (This work)			
T=593 K Conversion=7%	Contact time=1.3 s		
	Acrolein	CO_2	Others
(020) MoO_3 crystallites	99	—	1
Non-oriented MoO_3 crystallites	99	—	1
MoO_3 Powder (Ref. 34)			
T=593 K Conversion=100%			
	Acrolein	CO_2	Others
MoO_3 powder	98	2	0.1
MoO_3 powder (Ref. 35)			
T=593 K Conversion=100%	Contact time=4 s		
	Acrolein	CO_2	Others
MoO_3 powder	93	0.4	7

edge sharing by the loss of an oxygen atom. This is characterized by the formation of striations in the crystals. In this study, X-ray diffraction patterns of the used catalysts revealed no evidence for this phenomenon. The catalysts did exhibit a purple colored discoloration, probably from deposition of iodine. There was no change in activity as the catalysts were taken to high temperature and then brought down.

The selectivity results obtained here agree well with those in the work cited above (Table 4). In those investigations, conducted mainly at 593 K in the absence of oxygen, the main product was acrolein, with side products consisting of propylene, and traces of acrylic acid, acetaldehyde, 1,5-hexadiene and phenol. In this study the last three products were not observed, probably due to their further oxidation in the presence of oxygen. At higher temperatures substantial amounts of benzene were obtained. The observed product distribution at these temperatures are unlikely to be due to gas-phase free-radical reactions because of the absence of the characteristic products, propylene oxide and acetaldehyde.[38] In this study a lower conversion of propylene was obtained than in the previous work. At 593 K the conversion was 7% as opposed to 100% for the other measurements. This is probably due to the use of a significantly lesser quantity of catalyst than previously. This work used a total of 0.18 m^2, whereas the other studies used 5.3 m^2 and 8 m^2.

Burrington and Grasselli have indicated that allyl iodide does not produce free allyl radicals as suggested by the group of Haber. Rather they propose that allyl iodide adsorbs on MoO_3 prior to reaction. Whatever the mechanism, the crucial observation is that allyl iodide reacts much more readily than propylene by bypassing the difficult hydrogen atom abstraction step. An intermediate resembling adsorbed allyl radical is likely.

Crystal Face Specificity of Propylene Oxidation on MoO_3. Figure 9 reports the rate of acrolein formation on unsupported MoO_3 needles and powder. Table 3 takes part of this data at low temperature and compares it to findings obtained on a similar system, oriented MoO_3 crystallites supported on graphite.[10,11] The results in both studies are very similar, the selectivity to acrolein is higher on the non-oriented samples by a factor of about two. On the basis of this selectivity difference and a statistical analysis of exposed planes, Volta et al., concluded that the various planes of MoO_3 catalyze different reactions.[13]

A similar analysis can be made here using the estimated average dimensions of the powder and needle crystallites. From these dimensions it can be calculated that there is approximately four times more edge plane surface area on the powder than on the needles (Table 2). If these are the planes solely responsible for acrolein formation, as Volta et al., suggest, the results here are in qualitative agreement with this suggestion. This study finds that the powder is twice as selective as the needles in the oxidation of propylene, and the approximate factor of four can account for this. However, noting that it is difficult to accurately measure the quantity of exposed planes by electron microscopy and, furthermore, recognizing that the differences between samples is exceedingly small, we defer here the question of determining crystal face specificity by this type of analysis until a more definitive study is undertaken.

The low selectivity to the product of interest in propylene oxidation (<ca. 10%) raises the question of whether a possible greater crystal face specificity is erased by the combination of the high temperatures employed and the presence of the unselective total oxidation reaction. For this reason it is desirable to examine the behavior of more reactive probe molecules. Table 5 reports the results obtained in the allylic oxidation of a number of propylene analogues on oriented and unoriented samples of MoO_3. There is a notable trend of increasing overall selectivity toward allylic oxidation products as the allylic bond strength decreases. In addition, in comparing the basal and edge oriented samples, there is less

Table 5. Allylic Oxidation of Propylene Analogues

Molecule	Bond energy / kJ mol^{-1}	Selectivity/% Basal sample	Selectivity/% Edge sample	Selectivity ratio	Ref.
CH_2=CH-CH_2-H Propylene	361[39]	3	6	2	This work
CH_2=CH-CH(CH_3)-H 1-Butene	345[39]	9	12	1.3	Ref. 13[a,b]
CH_2=C(CH_3)-CH_2-H Isobutene	322[40]	27	36	1.3	Ref. 13[a,c]
CH_2=CH-CH_2-I Allyl iodide	184[41]	99	99	1	This work

a) Basal sample=85% (010) plane, 15% edge planes. b) Edge sample=55% (010) plane, 45% edge planes. c) Edge sample=61% (010) plane, 39% edge planes.

variability in the selectivities as the bond strength decreases. For propylene, 1-butene, isobutene, and allyl iodide oxidation the selectivities change by factors of only 2, 1.3, 1.3, and 1, respectively. This is understandable as those molecules whose allylic positions are easier to activate are expected to show lesser sensibility to the structure of the surface. Factors like the above are small in catalysis, and they suggest that allylic oxidation on MoO_3 is only slightly sensitive to the structure of the surface. However, the differences are reproducible[10,11] and do demonstrate trends, indicating a variability of the rate with the structure of the surface. Thus, we must recognize here a contribution of the structure to the reactivity, even though it is outside the confines of a range of variation of rate characteristic of structure-sensitive reactions.

Conclusion

Oriented crystallites of MoO_3 in the shape of needles and a random powder were used to investigate the partial oxidation of propylene and allyl iodide. Only a small difference in reactivity of both materials in propylene oxidation is observed, indicating that the reaction depends only slightly on the structure of the MoO_3.

The author thanks Dr. Leo Volpe for taking the scanning electron micrographs, Prof. Richard W. Gaver for the usage of the Cary 81 Raman spectrometer, Prof. Michel Boudart for extensive discussions, and Catalytica for permission to publish this work.

References

1) K. Tanaka and T. Okuhara, "Proc. 3rd Int. Conf. Molybdenum, The Chemistry and Uses of Molybdenum," ed by H. F. Barry and P. C. H. Mitchell, Climax Molybdenum Co., 1979, p. 170.
2) K. Tanaka and T. Okuhara, *J. Catal.*, **65**, 1 (1980).
3) K. Tanaka and T. Okuhara, *J. Catal.*, **78**, 155 (1982).
4) P. Berlowitz and H. H. Kung, *J. Am. Chem. Soc.*, **108**, 3533 (1986).
5) H. S. Taylor, *Proc. R. Soc. London, Ser. A*, **108**, 105 (1925).
6) M. Boudart, A. Aldag, J. E. Benson, N. A. Dougharty, and C. Girvin Harkins, *J. Catal.*, **6**, 92 (1966).
7) M. Boudart, *Adv. Catal.*, **20**, 153 (1969).
8) M. Boudart, "Proc. 6th Int. Cong. Catal.," London, 1976, Vol. 1, p. 1 ed by G. C. Bond, P. B. Wells, and F. C. Tomkins, Chemical Society, London, 1977.
9) J. C. Volta, W. Desquesnes, B. Moraweck, and G. Coudurier, *React. Kinet. Catal. Lett.*, **12**, 241 (1979).
10) J. C. Volta and B. Moraweck, *J. Chem. Soc., Chem. Commun.*, **1980**, 338.
11) J. C. Volta, W. Desquesnes, B. Moraweck, and J. M. Tatibouët, "Proc. 7th Int. Cong. Catal.," Tokyo, 1980, Part B. p. 1398, ed by T. Seiyama and K. Tanabe, Elsevier, Amsterdam, 1981.
12) J. C. Volta, M. Forissier, F. Theobald, and T. P. Pham, *Farad. Disc. Chem. Soc.*, **72**, 225 (1981).
13) J. C. Volta, J. M. Tatibouët, C. Phichitkul, and J. E. Germain, "Proc. 8th Int. Cong. Catal.," Berlin 1984, Vol. 4, p. 451, Verlag Chemie, 1984.
14) J. M. Tatibouët and J. E. Germain, *J. Catal.*, **72**, 375 (1981).
15) J. M. Tatibouët and J. E. Germain, *J. Chem. Res. (S)*, **1981**, 268.
16) J. M. Tatibouët and J. E. Germain, *J. Chem. Res. (M)*, **1981**, 3070.
17) F. Ohuchi and U. Chowdhry, "Proceedings of the 12th North American Thermal Analysis Society Conference," Paper #103, Williamsburg, Virginia, September 1983.
18) F. Ohuchi, L. E. Firment, U. Chowdhry, and A. Ferretti, *J. Vac. Sci. Technol.*, **A2**, 1022 (1984).
19) J. Ziółkowski, *J. Catal.*, **80**, 263 (1983).
20) J. N. Allison and W. A. Goddard, III, *J. Catal.*, **92**, 127 (1985).
21) L. Kihlborg, *Arkiv Kemi*, **21**, 357 (1963).
22) B. Wanklyn, *J. Crystal Growth*, **2**, 251 (1968).
23) C. R. Adams and T. J. Jennings, *J. Catal.*, **2**, 63 (1963).
24) C. R. Adams and T. J. Jennings, *J. Catal.*, **3**, 549 (1964).
25) W. M. H. Sachtler and N. H. de Boer, "Proc. 3rd Int. Cong. Catal," Amsterdam, 1964, Vol. I, p. 252, ed by W. M. H. Sachtler, G. C. A. Schuit and P. Zwietering, North Holland Publ. Co., Amsterdam, 1965.
26) J. Haber, B. Grzybowska, *J. Catal.*, **28**, 489 (1973).
27) J. Haber, M. Sochacka, B. Grzybowska, and A.

Goleobiowsky, *J. Mol. Catal.*, **1**, 35 (1975).
28) G. N. Keulks, *J. Catal.*, **19**, 232 (1970).
29) Y. Morooka, "Proc. Fifth Int. Cong. Catal.," Miami Beach, 1972, Vol. 2, p. 981, ed by J. W. Hightower, North Holland Publ. Co., Amsterdam-London, American Elsevier Co. Inc., New York, 1973.
30) L. Ya. Margolis, *Catal. Rev. Sci. Eng.*, **8**, 241 (1973).
31) A. Bielanski and J. Haber, *Catal. Rev. Sci. Eng.*, **19**, 1 (1979).
32) L. A. Kassatkina and G. K. Boreskov, *Zhur. Fiz. Khim.*, **29**, 455 (1959).
33) J. Haber, *Z. Chem.*, **13**, 241 (1973).
34) B. Grzybowska, J. Haber, and J. Janas, *J. Catal.*, **49**, 150 (1977).
35) J. D. Burrington and R. K. Grasselli, *J. Catal.*, **59**, 79 (1979).
36) P. L. Gai, "Proc. 3rd Int. Conf. Molybdenum, The Chemistry and Uses of Molybdenum," p. 143, ed by H. F. Barry and P. C. H. Mitchell, Climax Molybdenum Co., 1979.
37) P. L. Gai, *Philos. Mag. A*, **43**, 841 (1981).
38) J. H. Jones, T. E. Daubert, and M. R. Fenske, *Ind. Engl. Chem. Prod. Res. Develop.*, **8**, 196 (1969).
39) D. F. McMillen and D. M. Golden, *Annual Rev. Phys. Chem.*, **33**, 493 (1982).
40) V. I. Vedeneyev, L. V. Gurvich, V. N. Kondratyev, V. A. Medvedev, and Ye. L. Frakevich, "Bond Energies, Ionization Potentials and Electron Affinities," English translation by Scripta Technica Ltd., St. Martin's Press, New York (1966).
41) K. W. Egger and A. T. Cocks, *Helv. Chim. Acta*, **56**, Fasc. 5, 1516 (1973).